

# Enhancing Monomeric Sugar Production from Coconut Husk by FeCl<sub>3</sub>-assisted Hydrothermal Pretreatment and Enzymatic Hydrolysis

Candra Wijaya<sup>1</sup>, Ningsi Lick Sangadji<sup>1</sup>, Maktum Muharja<sup>1</sup>, Tri Widjaja<sup>1</sup>, Lieke Riadi<sup>2</sup>,  
Arief Widjaja<sup>1\*</sup>

<sup>1</sup>Department of Chemical Engineering, Faculty of Industrial Technology, Institut Teknologi Sepuluh Nopember, Surabaya 60111, Indonesia.

<sup>2</sup>Departement of Chemical Engineering, Faculty of Engineering, Universitas Surabaya (UBAYA), Jalan Raya Kalirungkut (Tenggilis), Surabaya 60293, Indonesia.

Received: 16<sup>th</sup> June 2025; Revised: 16<sup>th</sup> August 2025; Accepted: 18<sup>th</sup> August 2025

Available online: 2<sup>nd</sup> September 2025; Published regularly: October 2025



## Abstract

Coconut husk (CCH), an abundant agricultural byproduct of the coconut processing industry, holds significant potential as a renewable feedstock for monomeric sugar production. However, efficient fractionation remains a challenge due to its recalcitrant lignocellulosic structure. This study investigates FeCl<sub>3</sub>-assisted hydrothermal pretreatment (HTP) as a selective and scalable approach to enhance enzymatic hydrolysis efficiency and sugar recovery. The effects of FeCl<sub>3</sub> concentrations, temperatures, and unified of pretreatment conditions as combined hydrolysis factor (CHF) on biomass fractionation, modeling xylan dissolution, and monomeric sugar production were evaluated. Results indicate that 0.06 M FeCl<sub>3</sub> at 150 °C achieved the highest total monomeric sugar concentration of 7.364 g/L, an 11-fold increase compared to the non-catalyzed control (0.667 g/L) during HTP. This condition also facilitated 81.2% hemicellulose removal while minimizing cellulose and lignin degradation, thereby improving enzymatic digestibility. Furthermore, xylan hydrolysis also successfully developed with high correlation with unified CHF parameter. FeCl<sub>3</sub>-assisted HTP CCH coupled with enzymatic hydrolysis further enhanced overall sugar recovery, with a total monomeric sugar yield of 18.4 g per 100 g raw CCH, representing a 4.4-fold increase compared to hydrothermally pretreated CCH without FeCl<sub>3</sub>. These findings highlight FeCl<sub>3</sub>-assisted HTP as a promising, cost-effective strategy for biomass fractionation, supporting its integration into lignocellulosic biorefineries for bio-based product development.

Copyright © 2025 by Authors, Published by BCREC Publishing Group. This is an open access article under the CC BY-SA License (<https://creativecommons.org/licenses/by-sa/4.0>).

**Keywords:** Coconut husk; FeCl<sub>3</sub>; monomeric sugar; hydrothermal; enzymatic hydrolysis

**How to Cite:** Wijaya, C., Sangadji, N.L., Muharja, M., Widjaja, T., Riadi, L., Widjaja, A. (2025). Enhancing Monomeric Sugar Production from Coconut Husk by FeCl<sub>3</sub>-assisted Hydrothermal Pretreatment and Enzymatic Hydrolysis. *Bulletin of Chemical Reaction Engineering & Catalysis*, 20 (3), 535-552. (doi: 10.9767/bcrec.20444)

**Permalink/DOI:** <https://doi.org/10.9767/bcrec.20444>

## 1. Introduction

The depletion of fossil fuels and the rise in greenhouse gas emissions have accelerated the global demand for sustainable energy solutions [1,2]. Consequently, the development of alternative biofuel sources has become increasingly crucial, and lignocellulosic biomass, a widely available and renewable resource, has

garnered attention for its potential to produce biofuels and valuable biochemicals [3–6].

Lignocellulosic biomass is composed of cellulose, hemicellulose, and lignin, which can be fractionated into various chemical platforms, including monomeric sugars. These sugars can be further processed into biofuels, chemicals, and other high-value compounds [7–9]. Glucose, a key monomeric sugar obtained from the enzymatic hydrolysis of cellulose, can be fermented into bioethanol [10]. Meanwhile, hemicellulosic sugars, particularly xylose, are valuable for xylitol

\* Corresponding Author.

Email: arief.widjaja@its.ac.id (A. Widjaja)

production [11]. Xylitol has diverse applications in the food and pharmaceutical industries and commands a higher market price, approximately \$5 per kilogram compared to ethanol's \$0.5 per kilogram, due to its sweetness, low-calorie content, and health benefits, particularly in reducing the risk of dental caries [12]. Integrating xylitol production into a biorefinery framework can significantly enhance the economic feasibility of biomass utilization [13].

Coconut husk (CCH), a byproduct of coconut processing, is abundantly available in tropical regions such as Indonesia, where the country produces 17.3 million tons of coconut fruit annually, the highest globally [14]. This abundance presents a significant opportunity to utilize CCH as a valuable feedstock for biofuel and biochemical production. However, similar with other lignocellulosic biomasses, the structural complexity and recalcitrance of CCH pose challenges for its efficient conversion into fermentable sugars [15]. Effective fractionation and pretreatment methods are necessary to enhance the biorefinery process of cellulose and hemicellulose, as well as lignin, in order to maximize the yields of valuable products and mitigate the issue of agricultural waste disposal [16,17]. Despite this potential, the valorization of CCH remains underexplored, with a lack of comprehensive investigations about pretreatment strategies.

Pretreatment is a critical step in breaking down the recalcitrant structure of feedstocks like CCH, improving the accessibility of their sugars for conversion [18]. Traditional pretreatment methods, such as sulfuric acid hydrolysis, are highly corrosive and generate byproducts that may hinder downstream biofuel fermentation [19]. Harsh acid-based approaches can degrade carbohydrates, forming inhibitory compounds like furfural and 5-hydroxymethylfurfural, which negatively affect microbial growth and fermentation efficiency [20]. In contrast, metal salts, particularly ferric chloride  $\text{FeCl}_3$ , have emerged as promising alternatives.  $\text{FeCl}_3$  is a promising alternative due to its lower corrosivity, higher selectivity, and ability to enhance sugar yields while minimizing inhibitor formation [21,22]. Additionally, it maintains high catalytic activity at the same pH as mineral acids with reduced risk to biological systems [23–25]. Hydrothermal pretreatment (HTP) methods, combined with  $\text{FeCl}_3$  as a catalyst, have been effective in overcoming the HTP constraints of high energy demands, prolonged reaction times, and relatively low sugar yields [26]. This study hypothesizes that  $\text{FeCl}_3$ , a low-cost metal salt, enhances HTP by selectively catalyzing hemicellulose hydrolysis, preserving cellulose, reducing reaction temperatures, and increasing enzymatic hydrolysis efficiency. Furthermore, the

$\text{FeCl}_3$ -assisted HTP has the potential to improve the enzymatic digestibility of CCH by removing non-cellulosic components like hemicellulose and disrupting the integrity of cellulose, potentially leading to enhanced overall sugar yields [25,27]. However, the pretreatment of CCH using  $\text{FeCl}_3$ -assisted HTP remains unexplored, and a comprehensive understanding of key variables, such as temperature and  $\text{FeCl}_3$  concentration, is required.

Therefore, this study aims to investigate the effect of  $\text{FeCl}_3$ -assisted HTP on the fractionation of CCH and production of monomeric sugars. The impacts of temperature and  $\text{FeCl}_3$  concentration on the solubilization of hemicellulose and the subsequent enzymatic hydrolysis performance were systematically evaluated. In addition, compositional analysis and solid characterization of pretreated biomass were conducted to provide insights into the structural disruption mechanism. This work is expected to offer valuable information for developing effective catalytic pretreatment strategies to valorize CCH within the sugar-platform biorefinery.

## 2. Materials and Methods

### 2.1 Materials

The CCH biomass was sourced from a local traditional market in Surabaya City, Indonesia. It was washed, sun-dried, and mechanically ground to a particle size of 40–60 mesh. The metal salt catalyst, pure analysis-grade  $\text{FeCl}_3 \cdot 6\text{H}_2\text{O}$ , was obtained from Merck, Germany. The cellulase enzyme, derived from *Trichoderma reesei* and the rest of analytical-grade chemicals were purchased from Sigma-Aldrich, USA.

### 2.2. $\text{FeCl}_3$ -Assisted HTP

The HTP reactor and heating setup were adapted from a previous study [14,28]. To assess the effectiveness of enhancing sugar production, the metal salt-catalyzed HTP of CCH was carried out by varying the  $\text{FeCl}_3$  catalyst concentration from 0.02, 0.06, and 0.1 M, as well as the pretreatment temperature from 120, 150, and 180°C. The solid-to-liquid ratio and reaction time were maintained constant at 1:20 and 30 minutes for each experiment. For comparison, HTP without a catalyst was also conducted at 150°C to understand the enhancement with and without the catalyst. All experiments were performed in duplicate. After pretreatment, the liquid hydrolysate was separated from the solid residues by vacuum filtration for sugar analysis and solid characterization. The impact of temperature and catalyst concentration was statistically evaluated based on the sugar concentration of the HTP hydrolysate, CCH composition, and enzymatic hydrolysis of the pretreated CCH.

To further quantify the influence of pretreatment parameters on hemicellulose removal from coconut husk (CCH), a biphasic kinetic model incorporating the combined hydrolysis factor (CHF), serving as a modified severity factor, was proposed. This model characterizes the xylan depolymerization behavior through a series of rate expressions, as outlined in Equation (1):

$$\frac{dX_{res}}{dt} = -k(T, C, \dots)CX_{res} \quad (1)$$

where  $X_{res}$  represents the residual xylan content retained in the pretreated solid, while  $T$  is the reaction temperature (K),  $C$  denotes the  $\text{FeCl}_3$  concentration (mol/L). The reaction rate constant,  $k(T, C, \dots)$  is a function of temperature, catalyst concentration, specifically  $\text{FeCl}_3$  in this study, and other influencing factors. The rate constant ( $k$ ) was expressed using an Arrhenius-type formulation that incorporates the catalytic effect of  $\text{FeCl}_3$ , as shown in [29–31]:

$$k = \exp\left(\alpha - \frac{E_a}{RT} + \beta C\right) \quad (2)$$

Where  $E_a$  denotes the apparent activation energy (kJ/mol),  $R$  is the universal gas constant (8.314 J/mol·K), and  $\alpha$  and  $\beta$  are empirically fitted parameters. Based on this formulation, the CHF for a given reaction time  $t$  was defined as shown in Eq. (3):

$$CHF = \exp\left(\alpha - \frac{E_a}{RT} + \beta C\right) Ct \quad (3)$$

Xylan was assumed to consist of two distinct fractions: fast-hydrolyzing ( $X_f$ ) and slow-hydrolyzing ( $X_s$ ) components. The hydrolysis kinetics of each fraction were described by the following rate equations, as shown in Eqs. (4) & (5) [29,31,32]:

$$\frac{dX_f}{dt} = -kCX_f \quad (4)$$

$$\frac{dX_s}{dt} = -fkCX_s \quad (5)$$

Where  $f$  represents the ratio of the rate constants for slow- and fast-hydrolyzing xylan, while  $\theta$  denotes the initial fraction of slow-reacting xylan. By solving the corresponding differential equations, the residual xylan content can be expressed as a function of the CHF, as shown in Eq. (6):

$$X_{res} = (1 - \theta) \exp(-CHF) + \theta \exp(-fCHF) \quad (6)$$

The model was fitted to experimental data to estimate the kinetic parameters  $\alpha$ ,  $\beta$ ,  $E_a$ ,  $\theta$ , and  $f$ , thereby elucidating the effects of pretreatment conditions, particularly temperature and  $\text{FeCl}_3$

concentration, on xylan solubilization and overall pretreatment performance. The objective function  $F$  was minimized to achieve the best fit between the predicted and experimental values of residual xylan, as described below:

$$F = \sum_{i=1}^N (X_{res,i}^{\text{model}} - X_{res,i}^{\text{exp}})^2 \quad (7)$$

where  $N$  is the number of data,  $X_{res,i}^{\text{model}}$  and  $X_{res,i}^{\text{exp}}$  are the modeled and experimental residual xylan respectively. This objective function was minimized on MATLAB 2024a.

### 2.3. Enzymatic Hydrolysis

Enzymatic hydrolysis of coconut coir husk (CCH) was performed using a cellulase enzyme, following the procedure described by [33]. In this study, 0.5 grams of solid residues from raw or pretreated CCH were combined with a buffer solution containing citric acid and sodium citrate, adjusted to a pH of 4.8. Subsequently, 20 FPU/g of cellulase enzyme was added to the mixture. The reaction mixture was incubated in a shaker at 50 °C for 72 hours, with a rotational speed of 150 rpm. The saccharification yield was calculated using the Eq. (8) [34]:

$$\%Y_{EH} = \frac{\text{released glucose} \times 0.9 \text{ (gram)}}{\text{cellulose in substrate (gram)}} \times 100\% \quad (8)$$

where  $\%Y_{EH}$  is the enzymatic hydrolysis yield from hydrolysate.

### 2.4. Determination of Sugars in Liquid Hydrolysate and Solid Compositional Analysis

The hydrolysates from HTP, solid compositional hydrolysate, and enzymatic hydrolysis processes were analyzed using high-performance liquid chromatography (HPLC) to determine sugar content. A Thermo Scientific Vanquish Core HPLC (Thermo Scientific, USA) equipped with a HyperREZ XP Carbohydrate Pb++ column (8 μm, 300×7.7 mm) (Thermo Scientific, USA) and a refractive index (RI) detector was used. The HPLC conditions were set as follows: flow rate of 0.6 mL/min, temperature of 85°C, pressure of 9 bar, and HPLC-grade water as the mobile phase.

Compositional analysis of the biomass was performed using the NREL method [35]. This procedure involved hydrolyzing the biomass with concentrated sulfuric acid to quantify carbohydrate components (monomeric sugars) and determine the lignin fraction, including acid-soluble lignin (ASL) and acid-insoluble lignin (AIL).

The impact of HTP on the CCH biomass was also assessed. The removal of specific CCH components was calculated using the following Eq. (9):

$$R_i(\%) = \left(1 - \frac{\text{pretreated CCH component mass}_{(g)}}{\text{initial CCH component mass}_{(g)}}\right) \times 100\% \quad (9)$$

Where  $R_i$  represents the removal percentage of a specific CCH component  $i$  (hemicellulose, cellulose, or lignin).

## 2.5. Crystallinity, Morphology, and Functional Group Analyses of CCH

The impact of pretreatment variables on the crystallinity, morphology, and functional groups of CCH was investigated. The crystallinity of solid fractions, both hydrothermally pretreated and untreated CCH, was analyzed using X-ray diffraction (XRD) following Segal's method [36,37]. XRD measurements were performed with an X'Pert PRO (PAN-analytical BV, Netherlands) using Cu-K $\alpha$  radiation at 40 kV and 30 mA. The crystallinity index (CrI) was calculated using Eq. (10):

$$CrI (\%) = \frac{I_{002} - I_{am}}{I_{002}} \times 100\% \quad (10)$$

where  $I_{002}$  represents the intensity of the 002 cellulose diffraction plane at 22.6°, and  $I_{am}$  corresponds to the intensity of the amorphous cellulose region at 18°.

Scanning electron microscopy (SEM) (Hitachi FlexSEM 1000, Japan) was used to examine morphological changes in CCH following various pretreatments. Additionally, Fourier transform infrared (FTIR) spectroscopy (Agilent Cary 630 FTIR Spectrometer, USA) was employed to assess modifications in functional groups within the CCH samples.

## 2.6. Statistical Analysis

The effect of pretreatment temperature and FeCl<sub>3</sub> concentration was evaluated by ANOVA at a significance level of 0.05. Tukey's pairwise

comparison was performed to determine significant differences among the experimental groups.

In addition, the nonlinear regression model (Eq. 6) describing xylan hydrolysis was statistically evaluated. Model parameters ( $a$ ,  $E_a$ ,  $\beta$ ,  $\theta$ , and  $f$ ) were estimated using nonlinear least-squares fitting, and their significance was assessed using t-tests at a 95% confidence level. For each parameter, the estimated value, and p-value were reported. The overall goodness-of-fit of the model was determined using R<sup>2</sup>, while ANOVA of the regression (F-test) was used to verify the statistical validity of the model. All analyses were performed using MATLAB R2024a.

## 3. Results and Discussion

### 3.1. Effect of Temperature and FeCl<sub>3</sub> Concentration on Monomeric Sugar Production

The hydrolysates obtained from HTP under different pretreatment conditions were analyzed to evaluate the influence of temperature and FeCl<sub>3</sub> concentration on sugar production, as illustrated in Figure 1. The glucose concentration (Figure 1a) exhibited an increasing trend with temperature for FeCl<sub>3</sub> concentrations of 0.02 M and 0.06 M. Specifically, as the temperature

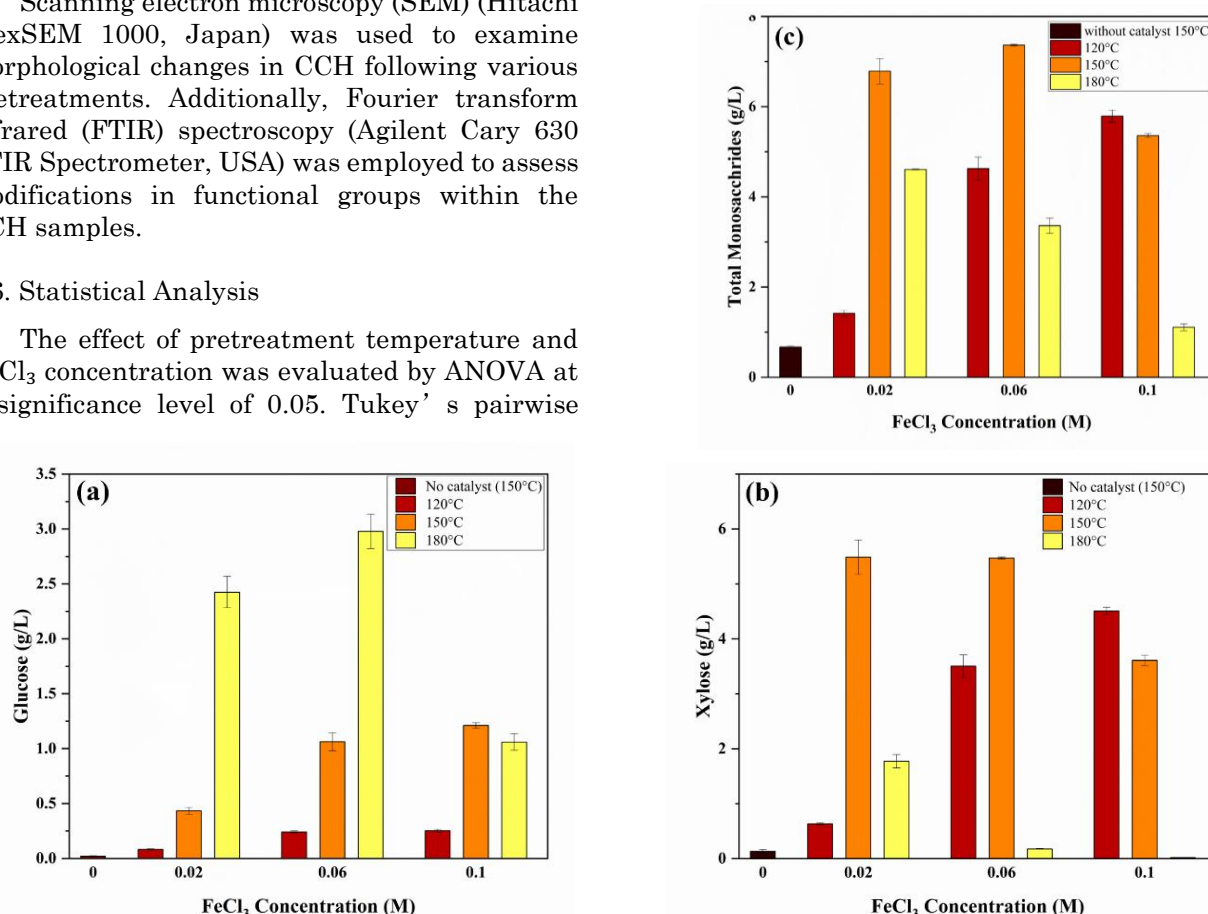


Figure 1. Effects of temperature and FeCl<sub>3</sub> concentration on glucose (a), xylose (b), and total monosaccharides (c) of HTP hydrolysates.

increased from 120 °C to 180 °C, the glucose concentration rose from 0.08 to 2.42 g/L for 0.02 M FeCl<sub>3</sub> and from 0.24 to 2.98 g/L for 0.06 M FeCl<sub>3</sub>. This enhancement can be attributed to the increased hydrolysis rate of glycosidic bonds in the cellulose structure of CCH at elevated temperatures, leading to greater glucose release [38]. However, a different trend was observed at 0.1 M FeCl<sub>3</sub>, where glucose concentration increased from 0.25 to 1.21 g/L as the temperature rose from 120 °C to 150 °C, followed by a decline to 1.06 g/L at 180 °C. This suggests that at higher FeCl<sub>3</sub> concentrations and elevated temperatures, glucose degradation becomes more pronounced. Previous studies have reported that harsh HTP temperatures promote sugar degradation, resulting in the formation of by-products such as 5-hydroxymethylfurfural (5-HMF) that further reduce glucose yield [39,40]. From a catalyst concentration perspective, glucose content increased with FeCl<sub>3</sub> concentration at each temperature. At 120 °C, glucose concentrations ranged from 0.08 to 0.25 g/L for 0.02–0.1 M FeCl<sub>3</sub>, while at 150 °C, the values ranged from 0.43 to 1.21 g/L. However, at 180 °C, glucose concentrations increased from 2.42 to 2.98 g/L for 0.02–0.06 M FeCl<sub>3</sub> but declined to 1.06 g/L at 0.1 M FeCl<sub>3</sub>, suggesting that excessive catalyst concentrations may accelerate glucose degradation into by-products [41]. Statistical analysis using ANOVA confirmed that both temperature and FeCl<sub>3</sub> concentration significantly influenced glucose production ( $p < 0.05$ ). Tukey's pairwise comparison further supported the observed trends. The comparison between catalyzed and uncatalyzed hydrolysis revealed a substantial improvement in glucose yield, increasing from 0.02 g/L without a catalyst to 2.98 g/L with FeCl<sub>3</sub>, representing a 149-fold enhancement. This finding suggests that the presence of FeCl<sub>3</sub> during HTP successfully enhances glucose production.

Xylose production also exhibited a significant improvement under FeCl<sub>3</sub>-assisted HTP, as depicted in Figure 1b. The xylose concentration increased with rising temperature but declined after 150 °C for 0.02 M and 0.06 M FeCl<sub>3</sub>. Specifically, at 0.02 M FeCl<sub>3</sub>, the xylose concentration increased from 0.63 g/L at 120 °C, peaked at 5.49 g/L at 150 °C, and then declined to 1.77 g/L at 180 °C. A similar trend was observed at 0.06 M FeCl<sub>3</sub>, where xylose concentration increased from 3.5 g/L at 120 °C, reached a maximum of 5.47 g/L at 150 °C, and dropped sharply to 0.18 g/L at 180 °C. However, at 0.1 M FeCl<sub>3</sub>, a different trend was observed, with a continuous decline in xylose concentration from 4.51 g/L at 120 °C to only 0.02 g/L at 180 °C. These results indicate that increasing temperature accelerates xylan hydrolysis into xylose, reaching an optimum temperature before degradation

occurs at harsher conditions. The earlier onset of degradation at 0.1 M FeCl<sub>3</sub> suggests that higher catalyst concentrations not only enhance xylan depolymerization but also promote xylose decomposition at elevated temperatures [42]. This is likely due to FeCl<sub>3</sub> acting as a catalyst for both hydrolysis and subsequent degradation reactions, leading to the formation of by-products under severe HTP conditions [43]. The effects of temperature and FeCl<sub>3</sub> concentration were further evaluated using ANOVA, which confirmed that both parameters significantly influenced xylose production ( $p < 0.05$ ). Unlike glucose, xylose release occurs at lower temperatures, suggesting that xylan is more readily hydrolyzed compared to cellulose. The highest xylose concentration achieved in this study was 1.83 times higher than the maximum glucose concentration, indicating that cellulose hydrolysis is more challenging due to its high crystallinity and stronger glycosidic bonds [12,44]. In contrast, xylan has an amorphous structure and a lower degree of polymerization, making it less recalcitrant and more susceptible to hydrolysis [45].

The total monosaccharides obtained from HTP, primarily composed of glucose and xylose, also followed by minor concentration of other hemicellulosic sugar such as galactose, arabinose, and mannose, presented in Figure 1c. The trend of total monosaccharide concentration closely follows that of xylose, as highest xylose yield was 1.83 times higher than highest glucose concentration. With the contribution of glucose, the total monosaccharide concentration exhibited an overall increase at higher temperatures (180 °C). The total monosaccharide concentration ranged from 1.11 to 7.36 g/L, with the highest concentration observed at 150 °C and 0.06 M FeCl<sub>3</sub>, whereas the lowest yield was recorded at 180 °C and 0.1 M FeCl<sub>3</sub>, representing the harshest conditions in this study. These results indicate that while moderate temperatures enhance biomass hydrolysis, excessive severity leads to sugar degradation, reducing overall sugar recovery. This aligns with previous findings where higher temperatures promote furfural and HMF formation, limiting monosaccharide accumulation [14,46]. The influence of FeCl<sub>3</sub> concentration was also evident, as higher catalyst loading (0.1 M) led to a rapid decline in sugar yield at 180 °C, suggesting that FeCl<sub>3</sub> not only facilitates hydrolysis but also enhances monosaccharide degradation at extreme conditions [42,47]. The statistical evaluation using ANOVA ( $p < 0.05$ ) confirmed that both temperature and FeCl<sub>3</sub> concentration significantly influenced total monosaccharide production, with Tukey's test highlighting 150 °C and 0.06 M FeCl<sub>3</sub> as the most effective condition. Compared to non-catalyzed HTP, FeCl<sub>3</sub>-assisted pretreatment demonstrated

superior sugar recovery, with a substantial increase in total monosaccharide yield (11 times higher). The findings suggest that  $\text{FeCl}_3$  selectively enhances hemicellulose hydrolysis, as reflected in the dominance of xylose over glucose in the hydrolysate. From an industrial perspective, the high sugar recovery at 150 °C and 0.06 M  $\text{FeCl}_3$  is particularly relevant for co-production of bioethanol and xylitol, biochemical synthesis, or biopolymer applications, where sugar selectivity is critical for downstream processes [12,48–50]. The observed trends provide insights into optimizing  $\text{FeCl}_3$ -assisted HTP for selective sugar fractionation, maximizing product recovery while minimizing sugar degradation.

### 3.2. Effect of $\text{FeCl}_3$ -HTP Conditions on Component Removal, Composition, and Xylan Hydrolysis via CHF Modeling

The impact of  $\text{FeCl}_3$  concentration and temperature on hemicellulose removal ( $R_H$ ) is presented in Figure 2a. The results indicate that hemicellulose solubilization increases with both  $\text{FeCl}_3$  concentration and temperature, with the highest removal observed at 180 °C across all catalyst concentration. At 0.02 M  $\text{FeCl}_3$ , hemicellulose removal increased from 32.03% at 120 °C to 74.59% at 150°C, reaching 90.12% at 180 °C, confirming the temperature-dependent depolymerization of hemicellulose. Similarly, at 0.06 M  $\text{FeCl}_3$ , removal increased from 52.68% at 120 °C to 81.93% at 150°C, peaking at 95.05% at 180 °C, demonstrating enhanced catalytic hydrolysis at moderate  $\text{FeCl}_3$  concentrations. At 0.1 M  $\text{FeCl}_3$ , hemicellulose removal was already 71.14% at 120 °C, increasing to 89.70% at 150 °C, but slightly decreasing to 92.87% at 180 °C. This suggests that higher  $\text{FeCl}_3$  concentrations accelerate hemicellulose hydrolysis at lower temperatures (120–150 °C), but beyond a certain threshold, increasing catalyst loading does not

significantly enhance solubilization. The minor difference in removal between 0.06 M and 0.1 M at 180 °C suggests a saturation point where hemicellulose is nearly depleted, with further  $\text{FeCl}_3$  addition yielding negligible benefits. This kind of effect was also observed from previous study as the temperature and concentration of catalyst increased, the hemicellulose removal approached completion, leaving small part of slow hydrolyzing xylan that was difficult to be removed [29,31]. ANOVA confirmed that temperature is the main factor in hemicellulose removal ( $p < 0.05$ ), with  $\text{FeCl}_3$  enhancing solubilization at moderate temperatures (150 °C). Tukey's test showed that increasing  $\text{FeCl}_3$  beyond 0.06 M at 180 °C did not significantly improve removal, identifying 0.06 M  $\text{FeCl}_3$  at 180 °C as the optimal condition (95.05% removal). These results highlight  $\text{FeCl}_3$ -assisted HTP as an effective method for selective hemicellulose fractionation in biorefinery applications.

The effect of temperature and  $\text{FeCl}_3$  concentration on cellulose removal ( $R_C$ ) is presented in Figure 2b. Unlike hemicellulose, cellulose exhibited greater resistance to hydrolysis, with low removal rates at 120 °C

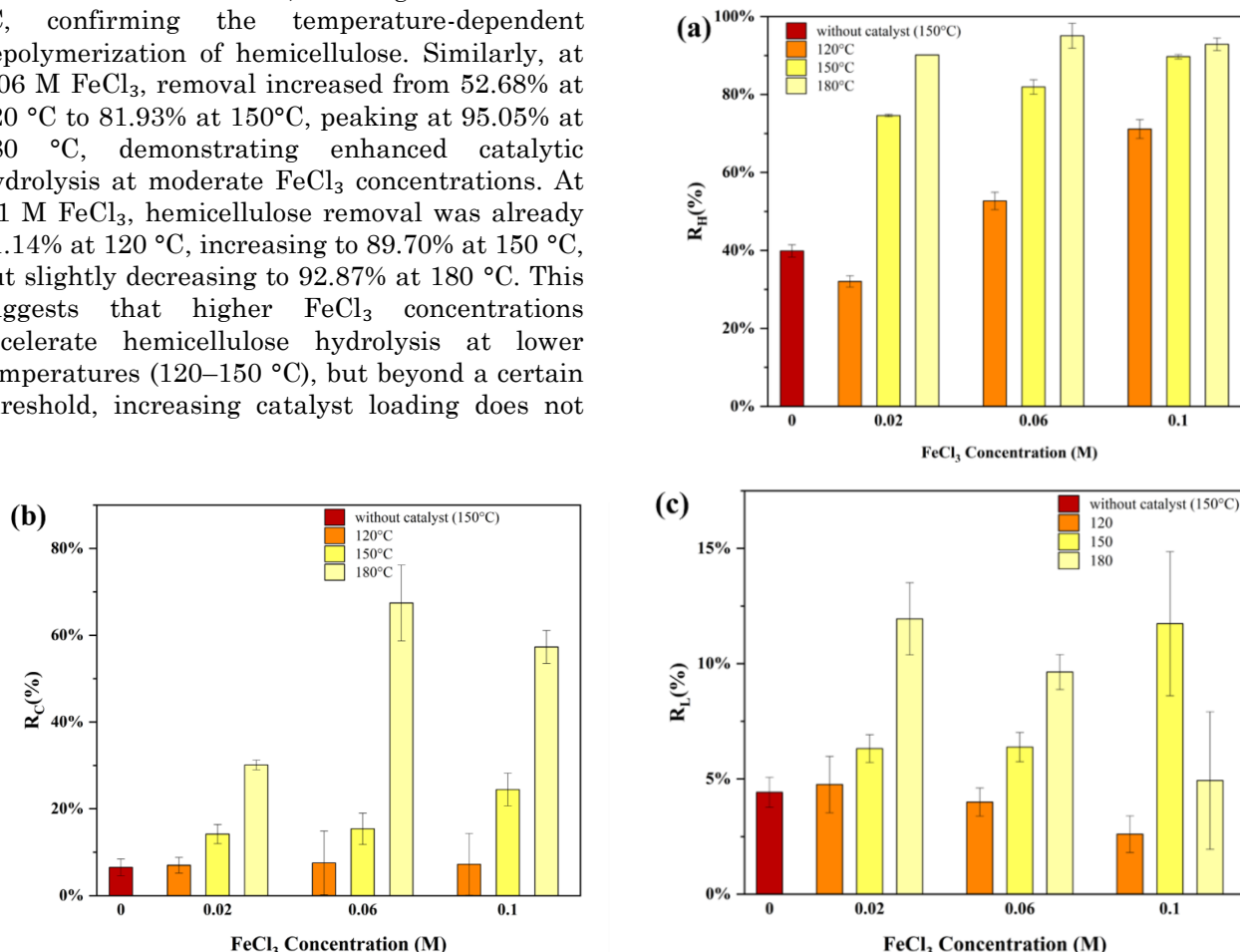


Figure 2. Effects of temperature and  $\text{FeCl}_3$  concentration on (a) hemicellulose removal ( $R_H$ ), (b) cellulose removal ( $R_C$ ), and (c) lignin removal ( $R_L$ ) of pretreated CCH.

across all  $\text{FeCl}_3$  concentrations. At 0.02 M  $\text{FeCl}_3$ , cellulose removal increased from 7.00% at 120 °C to 14.18% at 150 °C, reaching 30.10% at 180 °C, indicating gradual degradation with increasing severity. A similar pattern was observed at 0.06 M  $\text{FeCl}_3$ , where removal increased from 7.52% at 120 °C to 15.39% at 150 °C, before rising sharply to 67.42% at 180 °C, demonstrating enhanced depolymerization under high-temperature acidic conditions. At 0.1 M  $\text{FeCl}_3$ , cellulose removal increased from 7.22% at 120 °C to 24.43% at 150 °C, with 57.29% removal at 180 °C. Interestingly, cellulose removal at 0.1 M  $\text{FeCl}_3$  (57.29%) was slightly lower than at 0.06 M  $\text{FeCl}_3$  (67.42%) at 180 °C, suggesting possible secondary degradation or repolymerization effects limiting further solubilization [51]. ANOVA confirmed temperature as the main factor in cellulose removal ( $p < 0.0001$ ), with  $\text{FeCl}_3$  showing a significant effect ( $p < 0.005$ ). Tukey's test revealed a saturation point at 0.06 M  $\text{FeCl}_3$  and 180°C, where 67.42% cellulose removal was achieved without excessive degradation. These findings highlight  $\text{FeCl}_3$ -assisted HTP also can remove some portion of cellulose.

The effect of temperature and  $\text{FeCl}_3$  concentration on lignin removal ( $R_L$ ) is presented in Figure 2c. Compared to hemicellulose and cellulose, lignin removal remained low, confirming its higher structural resistance to hydrothermal conditions. At 120 °C, removal ranged from 2.60% (0.1 M  $\text{FeCl}_3$ ) to 4.76% (0.02 M  $\text{FeCl}_3$ ), with a slight increase at 150 °C, reaching 11.74% at 0.1 M  $\text{FeCl}_3$ . At 180 °C, removal peaked at 11.94% (0.02 M  $\text{FeCl}_3$ ), but decreased at higher  $\text{FeCl}_3$  concentrations (9.64% at 0.06 M, 4.93% at 0.1 M), suggesting potential lignin repolymerization or condensation [51–53]. ANOVA confirmed that temperature significantly influenced lignin removal ( $p < 0.0001$ ), while  $\text{FeCl}_3$  concentration had no significant effect ( $p = 0.1457$ ). The interaction effect ( $p = 0.0042$ ) suggests  $\text{FeCl}_3$  plays a minor role, becoming more relevant at higher temperatures. Tukey's post-hoc test indicated that while lignin solubilization increased between 120 °C and 180 °C, no significant difference was observed between 0.06 M and 0.1 M  $\text{FeCl}_3$  at 180 °C ( $p > 0.05$ ), confirming a saturation point where additional  $\text{FeCl}_3$  does not enhance lignin removal. These results indicate that  $\text{FeCl}_3$ -assisted HTP primarily targets hemicellulose and cellulose, with limited lignin solubilization. The increased lignin retention at higher  $\text{FeCl}_3$  concentrations may be beneficial for applications where lignin-enriched residues are desired, such as biocomposites, adsorbents, or bio-based materials [54,55].

The effects of  $\text{FeCl}_3$ -assisted HTP on hemicellulose, cellulose, and lignin composition of CCH are presented in Figure 3. The results demonstrate that hemicellulose was selectively

solubilized, cellulose was partially degraded under severe conditions, and lignin was relatively retained, leading to significant compositional shifts.

Hemicellulose content in raw CCH was 24.77%, which decreased progressively with increasing  $\text{FeCl}_3$  concentration and temperature. Without a catalyst at 150 °C, hemicellulose removal was moderate (17.29%), suggesting temperature alone contributes to partial solubilization. The addition of  $\text{FeCl}_3$  significantly enhanced hemicellulose degradation, particularly at higher concentrations and temperatures. At 120 °C, hemicellulose content was 17.22% at 0.02 M  $\text{FeCl}_3$  and 12.59% at 0.06 M  $\text{FeCl}_3$ , while at 0.1 M  $\text{FeCl}_3$ , it decreased further to 8.58%, indicating a concentration-dependent effect on hemicellulose solubilization. At 150 °C, hemicellulose removal became more pronounced, reducing to 7.22% at 0.02 M  $\text{FeCl}_3$ , 5.27% at 0.06 M  $\text{FeCl}_3$ , and 3.73% at 0.1 M  $\text{FeCl}_3$ , confirming increased hydrolysis with higher  $\text{FeCl}_3$  concentrations [29,31]. At 180 °C, hemicellulose was nearly depleted, reaching 3.13% at 0.06 M  $\text{FeCl}_3$  and 3.36% at 0.1 M  $\text{FeCl}_3$ , suggesting no further benefit in increasing  $\text{FeCl}_3$  beyond 0.06 M under high-temperature conditions.

Cellulose composition followed a different trend, showing an initial increase under mild pretreatment conditions due to preferential hemicellulose removal, but declining under harsher conditions. The raw CCH contained 38.30% cellulose, which slightly increased at 120 °C, reaching 43.16% at 0.02 M  $\text{FeCl}_3$ , 44.69% at 0.06 M  $\text{FeCl}_3$ , and 47.08% at 0.1 M  $\text{FeCl}_3$ , indicating minimal degradation at low temperatures. At 150 °C, cellulose content peaked at 47.54% at 0.06 M  $\text{FeCl}_3$ , while at 0.1 M  $\text{FeCl}_3$ , it remained high at 47.02%, confirming that moderate conditions preserve cellulose while

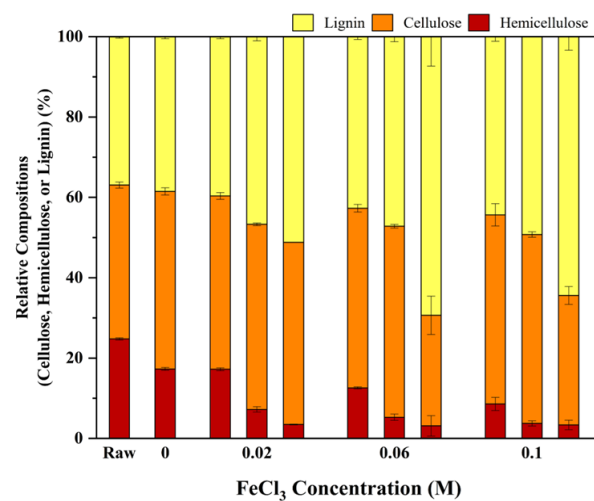


Figure 3. Effects of temperature and  $\text{FeCl}_3$  concentration on relative compositions of unpretreated (raw) and pretreated CCH.

solubilizing hemicellulose [38,56]. However, at 180°C, cellulose degradation became significant, with content decreasing to 27.51% at 0.06 M  $\text{FeCl}_3$  and 32.23% at 0.1 M  $\text{FeCl}_3$ , suggesting that while  $\text{FeCl}_3$  enhances selective hydrolysis, excessive catalyst concentrations do not further degrade cellulose at high temperatures [42,57]. This trend aligns with Figure 2b, where cellulose removal was significant at 180 °C, indicating  $\text{FeCl}_3$ -assisted pretreatment improves fractionation but should be optimized to minimize cellulose loss.

Lignin content exhibited a relative increase due to preferential hemicellulose and cellulose removal rather than extensive lignin solubilization. In raw CCH, lignin content was 36.93%, which increased across all pretreatment conditions as polysaccharides were removed. At 120°C, lignin content increased to 39.61% at 0.02 M  $\text{FeCl}_3$ , 42.71% at 0.06 M  $\text{FeCl}_3$ , and 44.33% at 0.1 M  $\text{FeCl}_3$ , showing minimal lignin removal. At 150 °C, lignin enrichment became more apparent, reaching 46.68% at 0.02 M  $\text{FeCl}_3$ , 47.18% at 0.06 M  $\text{FeCl}_3$ , and 49.24% at 0.1 M  $\text{FeCl}_3$ , confirming preferential degradation of other components. At 180 °C, lignin retention peaked at 51.96% at 0.06 M  $\text{FeCl}_3$  and 51.94% at 0.1 M  $\text{FeCl}_3$ , indicating no significant lignin degradation even at high  $\text{FeCl}_3$  concentrations. This trend, also observed in Figure 2c, confirms lignin's resistance to  $\text{FeCl}_3$ -assisted HTP, making further delignification necessary for specific applications.

ANOVA confirmed that temperature was the dominant factor influencing all components ( $p < 0.0001$ ), while  $\text{FeCl}_3$  concentration had a significant but secondary role, particularly in hemicellulose and cellulose fractionation. Tukey's post-hoc analysis showed significant differences in hemicellulose and cellulose composition between 120 °C and 180 °C, with no significant improvement beyond 0.06 M  $\text{FeCl}_3$  ( $p > 0.05$ ), indicating a catalyst saturation point. Lignin

content variations were mainly temperature-driven, with  $\text{FeCl}_3$  having minimal impact on lignin solubilization.

These results indicate that 0.06 M  $\text{FeCl}_3$  at 150 °C represents an optimal pretreatment condition, achieving substantial hemicellulose removal with minimal cellulose degradation and effective lignin preservation, features that are highly desirable for biorefinery processes targeting sugar recovery and lignin valorization. Further increasing the  $\text{FeCl}_3$  concentration to 0.1 M yielded no significant additional improvement, confirming 0.06 M as the most efficient catalyst dosage for maximizing biomass fractionation while maintaining operational feasibility.

Building on the effective xylan solubilization observed under  $\text{FeCl}_3$ -assisted hydrothermal conditions, the CHF was introduced as a unified parameter to represent the collective influence of temperature, reaction time, and  $\text{FeCl}_3$  concentration as represented in Figure 4. Model fitting based on Eq. (6) produced a high determination coefficient ( $R^2=0.98$ ), demonstrating strong predictive reliability and the fitting parameters were listed in Table 1. The predicted residual xylan values ( $X_{\text{res}}$ ) closely aligned with experimental data (Figure 4a), and the parity plot (Figure 4b) confirmed the model's accuracy, with most data points distributed along the 1:1 line. A sharp decline in residual xylan content was observed at  $\text{CHF} < 6$ , corresponding to rapid hydrolysis of the fast-reacting xylan fraction. Beyond this point, xylan solubilization plateaued, suggesting the persistence of more recalcitrant xylan embedded in the lignin-cellulose matrix. This biphasic behavior was well described by model parameters  $\theta$  and  $f$ , representing the initial fraction and relative rate constant of slow-hydrolyzing xylan, respectively. Similar solubilization trends have been reported

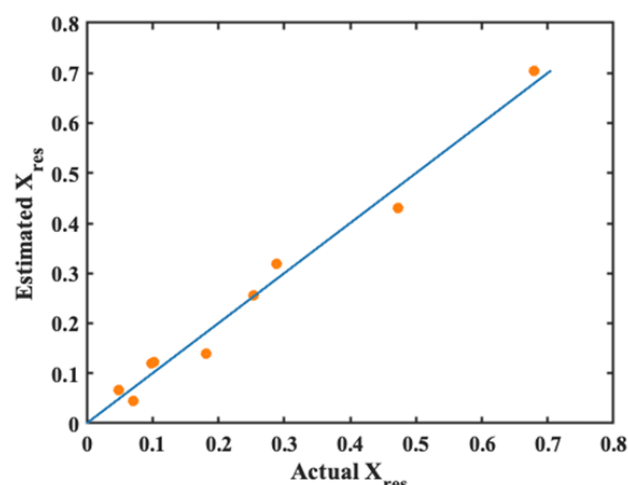
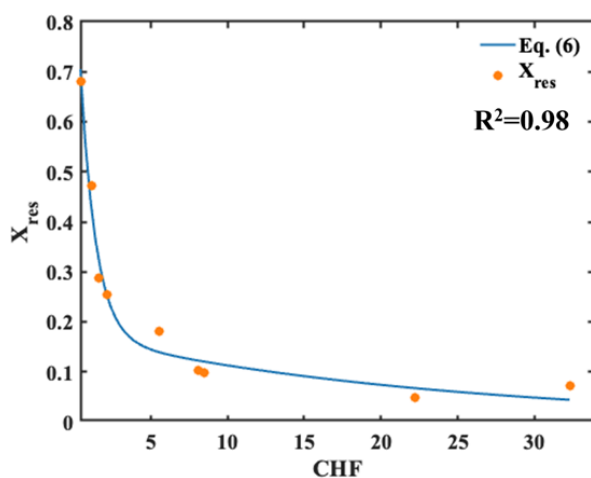


Figure 4. (a) Relationship between CHF and  $X_{\text{res}}$ , as modeled by Eq. (6); (b) Parity plot comparing actual and predicted values of  $X_{\text{res}}$ .

for both inorganic and organic acid pretreatments, where rapid early stage depolymerization is followed by a slower degradation phase [31,32].

The apparent activation energy ( $E_a$ ) for xylan hydrolysis was estimated at 73.3 kJ/mol, aligning with reported values for dilute acid pretreatment of densified corn stover (72.2 kJ/mol) and reflecting the intrinsic energy barrier associated with hemicellulose deconstruction. The catalytic role of  $\text{FeCl}_3$ , acting as a Lewis acid, likely enhances xylan depolymerization by polarizing coordinated water molecules and facilitating glycosidic bond cleavage [58]. For comparison, higher activation energies such as 97.90 kJ/mol have been reported for p-toluenesulfonic acid-pretreated poplar [59], highlighting how catalyst type and substrate characteristics influence the energy demand of hydrolysis reactions. Despite the absence of mechanical densification, the relatively low activation energy observed in this study further confirms the catalytic efficiency of  $\text{FeCl}_3$ . Overall, these findings reinforce CHF as a reliable and mechanistically grounded metric for describing pretreatment severity and predicting xylan solubilization behavior, providing valuable guidance for the design and optimization of lignocellulosic biomass fractionation strategies.

In addition, the ANOVA results for each regression coefficient are presented in Table 1. The F-values confirmed that the estimated parameters were statistically significant ( $p < 0.05$ ), indicating that each term contributed meaningfully to the model's predictive ability. This further validates the robustness of the nonlinear regression model or the biphasic model equation in describing xylan hydrolysis under varying pretreatment conditions. Despite the

absence of mechanical densification, the relatively low activation energy observed in this study further confirms the catalytic efficiency of  $\text{FeCl}_3$ . Overall, these findings reinforce CHF as a reliable and mechanistically grounded metric for describing pretreatment severity and predicting xylan solubilization behavior, providing valuable guidance for the design and optimization of lignocellulosic biomass fractionation strategies.

### 3.3. Solid Characterization of HTP- $\text{FeCl}_3$ Assisted CCH

The pretreatment impacts on residual CCH were examined using SEM, FTIR, and XRD for different temperatures and 0.06 M  $\text{FeCl}_3$  as selected catalyst concentration. These analyses provide insights into morphological modifications, functional group changes, and crystallinity variations, which influence the enzymatic hydrolysis efficiency of pretreated biomass.

The morphological changes in CCH following  $\text{FeCl}_3$ -assisted HTP were observed through SEM imaging (Figure 5a). Raw CCH exhibited a dense and compact fiber structure, indicating the

Table 1. Model parameters obtained from fitting Eq. (6) to CCH xylan hydrolysis data and ANOVA result.

Model parameters	Unit	Fitted value	F-value	p-value
$E_a$	kJ/mol	73.3	34.3844	0.0042
$\theta$	none	0.172	9.5712	0.0364
$f$	none	0.042	1.9245	0.2377
$\alpha$	none	22.17	35.3274	0.0040
$\beta$	L/mol	-3.38	1.2674	0.3232

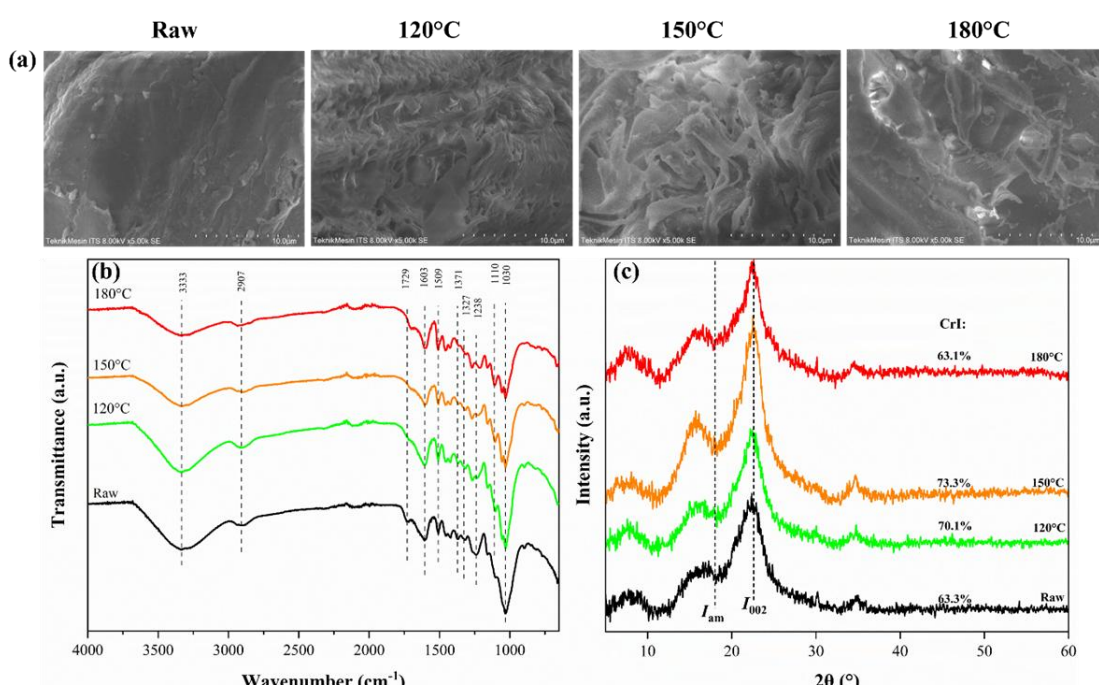


Figure 5. Solid characterization of pretreated CCH: (a) SEM, (b) FTIR, and (c) XRD. The effects of  $\text{FeCl}_3$ -assisted HTP on the structural and chemical characteristics.

presence of an intact lignocellulosic matrix with minimal porosity. After pretreatment at 120 °C, partial disruption of the fiber structure was observed, with an increase in surface roughness due to the removal of major hemicellulose component. More pronounced structural changes were evident at 150 °C, where the fibers appeared more separated and fragmented, suggesting enhanced solubilization of hemicellulose and lignin. At 180 °C, extensive fibrillation and disruption of the cell wall structure were observed, indicating significant hemicellulose removal and partial lignin degradation [56,60]. The increased surface porosity and fiber separation observed at higher pretreatment temperatures suggest improved enzymatic accessibility, which is essential for efficient saccharification [61].

The chemical transformations of FeCl<sub>3</sub>-assisted hydrothermally pretreated CCH were analyzed using FTIR to identify changes in functional groups associated with hemicellulose, cellulose, and lignin. The related reference of peaks and group assignment were summarized in Table 2. As shown in Figure 5b, a reduction in peak intensities was observed, confirming the selective removal of hemicellulose and modification of lignin during pretreatment. The broad absorption band at 3345 cm<sup>-1</sup>, attributed to hydrogen bonding interactions in hemicellulose, cellulose, and lignin, decreased after pretreatment, indicating the disruption of the lignocellulosic matrix and enhanced accessibility of cellulose. The 2907 cm<sup>-1</sup> peak, corresponding to C-H stretching in lignin, also declined, suggesting partial lignin degradation [62]. A significant decrease in the 1729 cm<sup>-1</sup> peak, assigned to carbonyl ester groups in lignin and acetyl groups in hemicellulose, confirmed hemicellulose

solubilization, particularly at 150 °C and 180 °C [3]. Similarly, the intensities of 1603 cm<sup>-1</sup> and 1507 cm<sup>-1</sup>, which correspond to aromatic ring stretching vibrations in lignin, were notably reduced, especially at 180 °C, indicating modifications in the lignin structure. Further evidence of hemicellulose removal was observed in the disappearance of peaks at 1371 cm<sup>-1</sup>, 1327 cm<sup>-1</sup>, and 1238 cm<sup>-1</sup>, representing C-H, O-H, and C-O bond vibrations commonly found in hemicellulose [14,63]. The drastic reduction of these peaks at higher temperatures suggests extensive hemicellulose solubilization under FeCl<sub>3</sub>-assisted hydrothermal conditions. These results confirm that FeCl<sub>3</sub>-assisted HTP effectively removes hemicellulose while modifying lignin, thereby increasing cellulose accessibility for enzymatic hydrolysis. The observed changes in functional groups are consistent with compositional analysis results, further validating the efficiency of the pretreatment process.

XRD analysis was conducted to evaluate changes in the crystallinity index (CrI) of CCH following FeCl<sub>3</sub>-assisted HTP (Figure 5c). The CrI was calculated by the intensity of cellulose crystalline phase I<sub>002</sub> ( $2\theta=22.6^\circ$ ) and amorphous peak (I<sub>am</sub>,  $2\theta=18^\circ$ ) [14]. The CrI of raw CCH was 63.3%, which increased to 70.1% after pretreatment at 120 °C, indicating partial removal of amorphous hemicellulose. A further increase in CrI was observed at 150 °C (73.3%), suggesting that hemicellulose degradation was maximized while cellulose integrity was preserved. However, at 180 °C, the CrI decreased to 63.1%, likely due to excessive cellulose degradation under severe conditions. These findings suggest that FeCl<sub>3</sub>-assisted HTP effectively enhances the crystallinity of CCH by selectively removing amorphous hemicellulose while preserving cellulose structure at moderate conditions. However, excessive pretreatment severity may lead to structural degradation, which could potentially increase the enzymatic digestibility of cellulose components in pretreated CCH [60,64].

The solid characterization results indicate that FeCl<sub>3</sub>-assisted HTP effectively modifies the structure of CCH, leading to hemicellulose removal, lignin modification, and cellulose disruption. These findings demonstrate the potential of FeCl<sub>3</sub>-assisted HTP as a viable strategy for improving lignocellulosic biomass fractionation and monomeric sugar production.

#### 3.4. Enzymatic Hydrolysis Evaluation of Pretreated CCH

The enzymatic hydrolysis performance of FeCl<sub>3</sub>-assisted hydrothermally pretreated CCH was evaluated, and the results are presented in Figure 6. The raw CCH had the lowest enzymatic

Table 2. FTIR peak spectrum and functional group.

Peak (cm <sup>-1</sup> )	Functional Group	Refs.
3333	Hydrogen bonding interactions within and between molecules in hemicellulose, cellulose, and lignin.	[62]
2907	Aliphatic C-H stretching was found in lignin.	[62]
1729	Carbonyl ester groups in lignin or acetyl groups in hemicelluloses.	[3].
1603	Aromatic ring stretching vibrations characteristic of lignin.	[56]
1509	Additional aromatic ring stretching vibrations observed in lignin.	[56]
1371	Presence of C-H, O-H, or C-O bonds, commonly found in hemicelluloses.	[56,63]
1327	C-H, O-H, or C-O bond vibrations associated with hemicelluloses.	[56,63]
1238	Characteristic stretching of C-H, O-H, or C-O bonds in hemicelluloses.	[56,63]

hydrolysis yield (6.79%), while HTP at 150 °C without FeCl<sub>3</sub> provided a slight improvement (7.02%), indicating limited effectiveness of heat alone in enhancing enzymatic digestibility. In contrast, FeCl<sub>3</sub>-assisted HTP significantly improved %Y<sub>EH</sub>, with the highest yield (19.28%) observed at 180 °C and 0.1 M FeCl<sub>3</sub>, representing a 2.84-fold increase over raw CCH. The effect of FeCl<sub>3</sub> concentration was temperature dependent. At 120 °C, %Y<sub>EH</sub> remained low (6.23%–7.21%) with no significant difference from the raw CCH. At 150 °C, FeCl<sub>3</sub> improved hydrolysis (9.35% at 0.02 M, 9.45% at 0.06 M), but declined at 0.1 M (8.20%). The most significant enhancement was observed at 180 °C, where %Y<sub>EH</sub> increased from 12.67% (0.02 M FeCl<sub>3</sub>) to 17.89% (0.06 M FeCl<sub>3</sub>), peaking at 19.28% (0.1 M FeCl<sub>3</sub>). Statistical analysis confirmed that temperature had the strongest effect ( $p < 0.0001$ ), followed by FeCl<sub>3</sub> concentration ( $p = 0.0036$ ), with a significant interaction ( $p = 0.0025$ ). Post hoc analysis showed higher temperatures significantly increased saccharification yield, while FeCl<sub>3</sub> beyond 0.06 M provided no further benefits ( $p > 0.05$ ) and may cause cellulose degradation. Prominent effect of temperature in enzymatic hydrolysis yield was also reported at somewhere else [42].

These trends align with FTIR, XRD, and SEM analyses, which confirm that FeCl<sub>3</sub>-assisted HTP enhances enzymatic digestibility by selectively removing hemicellulose and modifying lignin, leading to higher crystallinity and improved cellulose accessibility. FTIR (Figure 5) indicates a reduction in hemicellulose-related peaks (1371 cm<sup>-1</sup>, 1327 cm<sup>-1</sup>, 1238 cm<sup>-1</sup>), while XRD shows increased CrI due to reduced amorphous fractions. SEM images (Figure 5) reveal a more fragmented and porous structure, facilitating enzyme penetration [3,65].

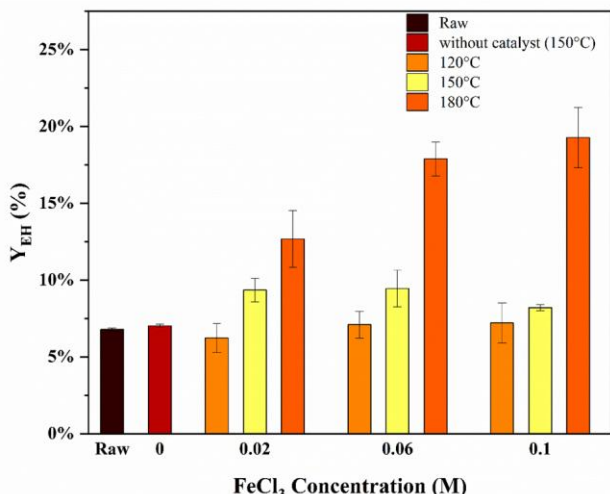


Figure 6. Effects of temperature and FeCl<sub>3</sub> concentration on enzymatic hydrolysis yield of unpretreated (raw) and pretreated CCH.

Overall, FeCl<sub>3</sub>-assisted HTP significantly improves enzymatic digestibility, with temperature playing the dominant role and FeCl<sub>3</sub> enhancing hydrolysis efficiency up to an optimal concentration of 0.06 M. The highest %Y<sub>EH</sub> (19.28%) at 180 °C and 0.1 M FeCl<sub>3</sub> demonstrates the potential of this approach for biomass saccharification, supporting its application in bioconversion processes.

### 3.5. Mass Balance Analysis and Comparative Evaluation of Pretreatment Performance

To assess the overall enhancement of FeCl<sub>3</sub>-assisted HTP on CCH sugar production, a mass balance analysis was conducted across multiple conditions (120–180 °C, 0.02–0.1 M FeCl<sub>3</sub>). Among these, 150 °C, 0.06 M FeCl<sub>3</sub> was identified as the most effective condition, balancing high monomeric sugar recovery with cellulose retention. Figure 7 summarizes the total monomeric sugar recovered from both HTP and enzymatic hydrolysis on a 100 g raw CCH basis, demonstrating that FeCl<sub>3</sub> catalysis enhances hemicellulose solubilization while maintaining enzymatic digestibility of the pretreated solids. This condition improves hydrolysis efficiency without requiring extreme temperatures (>180 °C), reducing both operational energy input and unwanted degradation of fermentable sugars [66].

The process mass balance calculation was demonstrated for selected optimal condition in Figure 8, provides further insights into the redistribution of biomass fractions through FeCl<sub>3</sub>-HTP and enzymatic hydrolysis. From 100 g of raw CCH, 28.54 g was solubilized, predominantly comprising xylose-rich hydrolysates (10.94 g xylose), glucose (2.12 g), and other sugars (1.66 g), leading to a total monomeric sugar yield of 14.72 g. The remaining pretreated CCH (71.46 g)

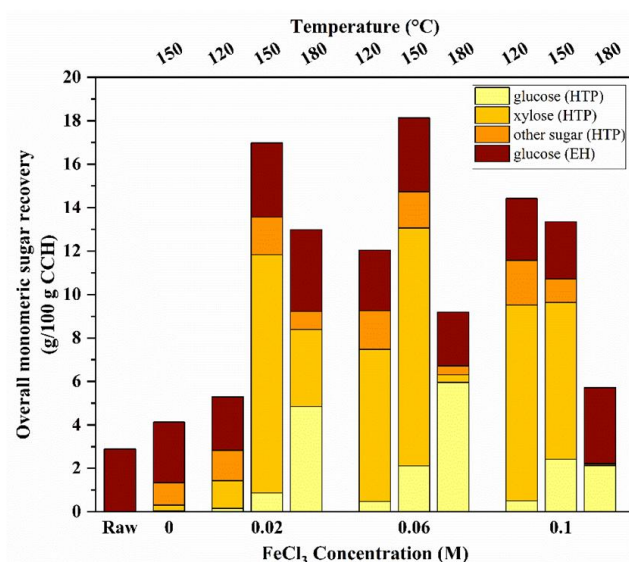


Figure 7. Overall monomeric sugar recovery of CCH from HTP and enzymatic hydrolysis (EH).

retained 4.48 g hemicellulose, 32.41 g cellulose, and 34.57 g lignin, ensuring that cellulose was preserved for enzymatic hydrolysis. Subsequent enzymatic hydrolysis released an additional 3.4 g of glucose, resulting in a cumulative monomeric sugar recovery of 18.12 g per 100 g of raw CCH. Higher 4.4 times than hydrothermal without catalyst. These findings highlight the synergistic role of  $\text{FeCl}_3$ -assisted pretreatment, where hemicellulose hydrolysis is facilitated while glucose from cellulose also recovered in subsequent enzymatic hydrolysis process [67].

The industrial applicability of  $\text{FeCl}_3$ -HTP is further supported by its mild reaction conditions and controlled depolymerization effects, making it a viable approach for large-scale co-production of bioethanol and polyols, and biochemical production [45,50]. To assess the effectiveness of  $\text{FeCl}_3$ -assisted HTP and EH in fractionating CCH, a comparative evaluation against previous studies was conducted and summarized in Table 3. The monomeric sugar recovery per 100 g raw CCH was used as a key performance indicator to determine the efficiency of various pretreatment approaches. Among the methods studied,  $\text{FeCl}_3$ -assisted HTP & EH (this study) at 150 °C, 0.06 M  $\text{FeCl}_3$  for 30

min demonstrated the highest monomeric sugar yield (18.4 g/100 g CCH), while maintaining a relatively short processing time and low temperature requirement, making it a promising candidate for large-scale biorefinery applications [68,69].

Conventional HTP has been widely used for lignocellulosic biomass fractionation, relying solely on high-temperature water treatment to solubilize hemicellulose and disrupt lignin networks. However, HTP at 259 °C for 30 min [70] only achieved 3.39 g/100 g CCH of monomeric sugar recovery, highlighting its inefficiency as a standalone method. The high temperature requirement not only increases energy consumption but also promotes sugar degradation, forming inhibitory compounds like furfural and 5-HMF, which negatively affect enzymatic hydrolysis and fermentation [3,71]. While HTP remains a chemical-free approach, its low sugar recovery and risk of thermal degradation limit its feasibility for industrial applications [72].

In an attempt to enhance lignin disruption and enzymatic digestibility, SDS-assisted HTP was introduced, incorporating 3% sodium dodecyl

Table 3. Overall monomeric sugar recovery of CCH from HTP and enzymatic hydrolysis (EH). (HT: hydrothermal; HTP: HTP; DES: deep eutectic solvent; EH: enzymatic hydrolysis; SDS: sodium dodecyl sulphate).

Process	Conditions	Monomeric sugar recovery (per 100 g raw CCH)	Refs.
HTP	259 °C, 30 min	3.39	[70]
SDS assisted-HTP	170 °C, 1 h, 3% SDS	12.3	[73]
HT-DES pretreatment & EH	HT: 210.7 °C, 77.9 min DES: 120 °C, 6 h	16.4	[14]
$\text{FeCl}_3$ -assisted HTP & EH	150 °C, 0.06 M $\text{FeCl}_3$ , 30 min	18.4	This study

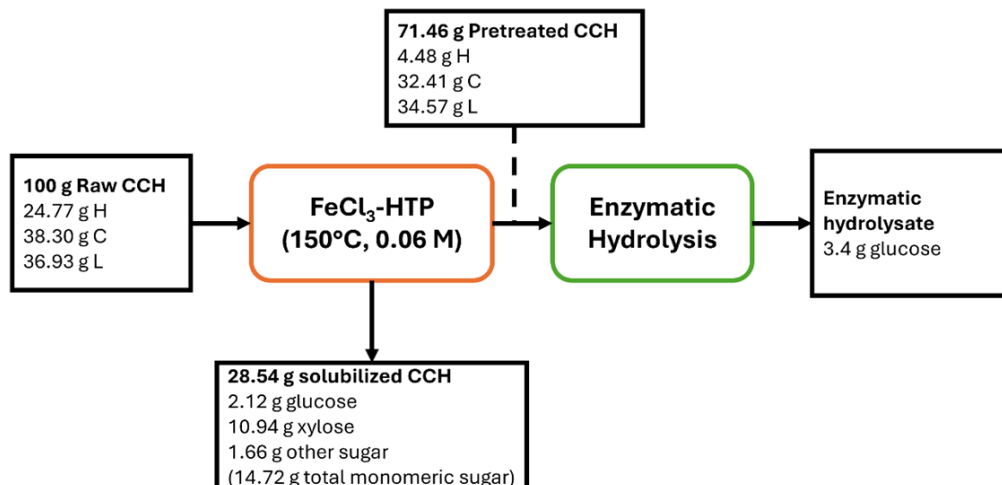


Figure 8. Process mass balance of  $\text{FeCl}_3$ -assisted HTP and enzymatic hydrolysis.

sulfate (SDS) at 170 °C for 1 hour [73]. This method significantly increased monomeric sugar recovery to 12.3 g/100 g CCH, demonstrating the effectiveness of surfactants in breaking lignin-carbohydrate complexes. However, the introduction of SDS raises environmental and cost concerns, as synthetic surfactants require proper chemical disposal or recovery systems. Additionally, residual SDS in hydrolysates could interfere with downstream microbial fermentation processes, making it less favorable for bioethanol production [74].

A more recent approach, hydrothermal-deep eutectic solvent (HT-DES) pretreatment followed by enzymatic hydrolysis [14], sought to combine hydrothermal and green solvent-based fractionation techniques. This two-step process (HT at 210.7°C for 77.9 min, followed by DES treatment at 120°C for 6 h) resulted in a monomeric sugar recovery of 16.4 g/100 g CCH, demonstrating improved fractionation efficiency. The addition of DES facilitated lignin dissolution, allowing for better sugar retention during enzymatic hydrolysis. However, the lengthy processing time (over 7 hours in total) and additional DES solvent preparation step reduce its scalability for industrial applications. While DES is considered a greener alternative to acid-based pretreatment, its cost, solvent recycling challenges, and prolonged reaction times hinder widespread adoption in large-scale operations [75].

In contrast,  $\text{FeCl}_3$ -assisted HTP & EH in this study achieved the highest monomeric sugar yield (18.4 g/100 g CCH) under milder conditions (150°C, 0.06 M  $\text{FeCl}_3$ , 30 min), surpassing previous methods in both efficiency and practicality. The  $\text{FeCl}_3$  catalyst selectively hydrolyzes hemicellulose, enhancing xylose and glucose release while preserving cellulose integrity, leading to higher enzymatic digestibility compared to conventional HTP. Unlike SDS-assisted HTP,  $\text{FeCl}_3$  does not introduce surfactant waste, making it a more environmentally friendly approach. Additionally, unlike HT-DES,  $\text{FeCl}_3$ -HTP operates under a single-step process with shorter reaction times, reducing processing complexity and operational costs. Despite these advantages,  $\text{FeCl}_3$ -assisted HTP still presents certain challenges that warrant further investigation. The reuse and recovery of  $\text{FeCl}_3$  should be optimized to minimize catalyst consumption and reduce operational costs. Additionally, excess Fe ions in hydrolysates must be carefully managed to prevent contamination, particularly in downstream fermentation processes [71, 76]. Future research should focus on catalyst recycling strategies and techno-economic assessments to further enhance the industrial feasibility of  $\text{FeCl}_3$ -based fractionation.

Overall, the findings suggest that  $\text{FeCl}_3$ -assisted HTP & EH offers a highly effective and scalable approach for lignocellulosic biomass fractionation, outperforming conventional hydrothermal and surfactant-assisted methods in sugar recovery, processing efficiency, and environmental sustainability. By combining high sugar yield, short processing time, and minimal chemical waste,  $\text{FeCl}_3$ -HTP presents a promising alternative for biofuel and biochemical production while maintaining cost-effective and sustainable biorefinery operations.

#### 4. Conclusions

This study demonstrated that  $\text{FeCl}_3$ -assisted HTP promoted the fractionation of coconut husk by enhancing hemicellulose solubilization while preserving cellulose in a more accessible form. The effects of temperature and  $\text{FeCl}_3$  concentration were systematically evaluated, with optimal conditions leading to selective hemicellulose removal and improved enzymatic hydrolysis efficiency. Compositional analysis and solid characterization using FTIR, XRD, and SEM confirmed structural disruption of hemicellulose and increased cellulose accessibility, which facilitated higher monomeric sugar yields. Overall, the findings provide insights into the role of  $\text{FeCl}_3$  as a catalytic aid in hydrothermal pretreatment for improving sugar production from lignocellulosic biomass.

#### Acknowledgments

The authors gratefully acknowledge the financial support from the Ministry of Education, Culture, Research, and Technology, Indonesia, through the PMDSU scholarship. We also extend our sincere appreciation to the Biochemical Technology Laboratory at Institut Teknologi Sepuluh Nopember, Surabaya, for providing the essential facilities that enabled the completion of this study.

#### Credit Author Statement

Author Contributions: Candra Wijaya: Conceptualization, Investigation, formal analysis, and Writing – original draft; Ningsi Lick Sangadji: Writing – review & editing; Maktum Muharja: Writing – review & editing; Tri Widjaja: Supervision, Writing – review & editing; Lieke Riadi Supervision: Writing – review & editing; and Arief Widjaja: Conceptualization, Data Curation, Writing – review & editing, Supervision, Project Administration. All authors have read and agreed to the published version of the manuscript.

## References

[1] Rodríguez-Rebelo, F., Rodríguez-Martínez, B., Del-Río, P.G., Collins, M.N., Garrote, G., Gullón, B. (2024). Assessment of deep eutectic solvents (DES) to fractionate Paulownia wood within a biorefinery scheme: Cellulosic bioethanol production and lignin isolation. *Industrial Crops and Products*, 216, 117220. DOI: 10.1016/j.indcrop.2024.118761.

[2] Rathour, R.K., Behl, M., Dhashmana, K., Sakhija, D., Ghai, H., Sharma, N., Meena, K.R., Bhatt, A.K., Bhatia, R.K. (2023). Non-food crops derived lignocellulose biorefinery for sustainable production of biomaterials, biochemicals and bioenergy: A review on trends and techniques. *Industrial Crops and Products*, 204, 117220. DOI: 10.1016/j.indcrop.2023.117220.

[3] Gundupalli, M.P., Tantayotai, P., Panakkal, E.J., Chueto, S., Kirdponpattara, S., Thomas, A.S.S., Sharma, B.K., Sriariyanun, M. (2022). Hydrothermal pretreatment optimization and deep eutectic solvent pretreatment of lignocellulosic biomass: An integrated approach. *Bioresource Technology Reports*, 17, 100957. DOI: 10.1016/j.bioteb.2022.100957.

[4] Zhang, Y., Ding, Z., Shahadat Hossain, M., Maurya, R., Yang, Y., Singh, V., Kumar, D., Salama, E.S., Sun, X., Sindhu, R., Binod, P., Zhang, Z., Kumar Awasthi, M. (2023). Recent advances in lignocellulosic and algal biomass pretreatment and its biorefinery approaches for biochemicals and bioenergy conversion. *Bioresource Technology*, 367, 128281. DOI: 10.1016/j.biortech.2022.128281.

[5] Yaashikaa, P.R., Senthil Kumar, P., Varjani, S. (2022). Valorization of agro-industrial wastes for biorefinery process and circular bioeconomy: A critical review. *Bioresource Technology*, 343, 126126. DOI: 10.1016/j.biortech.2021.126126.

[6] Basak, B., Kumar, R., Bharadwaj, A.V.S.L.S., Kim, T.H., Kim, J.R., Jang, M., Oh, S.E., Roh, H.S., Jeon, B.H. (2023). Advances in physicochemical pretreatment strategies for lignocellulose biomass and their effectiveness in bioconversion for biofuel production. *Bioresource Technology*, 369, 128413. DOI: 10.1016/j.biortech.2022.128413.

[7] Saini, R., Singhania, R.R., Patel, A.K., Chen, C.W., Piechota, G., Dong, C. Di (2024). Sustainable production of cellulose and hemicellulose-derived oligosaccharides from pineapple leaves: Impact of hydrothermal pretreatment and controlled enzymatic hydrolysis. *Bioresource Technology*, 398, 130526. DOI: 10.1016/j.biortech.2024.130526.

[8] Domínguez, E., Río, P.G. del, Romaní, A., Garrote, G., Domingues, L. (2021). Hemicellulosic Bioethanol Production from Fast-Growing Paulownia Biomass. *Processes*, 9(1), 173. DOI: 10.3390/pr9010173.

[9] Peng, F., Peng, P., Xu, F., Sun, R.-C. (2012). Fractional purification and bioconversion of hemicelluloses. *Biotechnology Advances*, 30(4), 879–903. DOI: 10.1016/j.biotechadv.2012.01.018.

[10] Gao, H., Wang, Y., Yang, Q., Peng, H., Li, Y., Zhan, D., Wei, H., Lu, H., Bakr, M.M.A., EI-Sheekh, M.M., Qi, Z., Peng, L., Lin, X. (2021). Combined steam explosion and optimized green-liquor pretreatments are effective for complete saccharification to maximize bioethanol production by reducing lignocellulose recalcitrance in one-year-old bamboo. *Renewable Energy*, 175, 1069–1079. DOI: 10.1016/j.renene.2021.05.016.

[11] Felipe Hernández-Pérez, A., de Arruda, P.V., Sene, L., da Silva, S.S., Kumar Chandel, A., de Almeida Felipe, M. das G. (2019). Xylitol bioproduction: state-of-the-art, industrial paradigm shift, and opportunities for integrated biorefineries. *Critical Reviews in Biotechnology*, 39(7), 924–943. DOI: 10.1080/07388551.2019.1640658.

[12] Feng, J., Techapun, C., Phimolsiripol, Y., Phongthai, S., Khemacheewakul, J., Taesuwan, S., Mahakuntha, C., Porninta, K., Htike, S.L., Kumar, A., Nunta, R., Sommanee, S., Leksawasdi, N. (2024). Utilization of agricultural wastes for co-production of xylitol, ethanol, and phenylacetylcarbinol: A review. *Bioresource Technology*, 392, 129926. DOI: 10.1016/j.biortech.2023.129926.

[13] Clauser, N.M., Fit, C.G., Cardozo, R.E., Rivaldi, J.A., Felissia, F.E., Area, M.C., Vallejos, M.E. (2024). Technical, Economic and Environmental Assessment of Xylitol Production in a Biorefinery Platform Toward a Circular Economy. *Sustainability*, 16(10770), 1–21. DOI: 10.3390/su162310770 Academic.

[14] Wijaya, C., Sangadji, N.L., Muharja, M., Widjaja, T., Riadi, L., Widjaja, A. (2025). An integrated green fractionation of coconut husk: Hydrothermal and deep eutectic solvent pretreatment for enhanced sugar and lignin production. *Bioresource Technology Reports*, 29, 102078. DOI: 10.1016/j.bioteb.2025.102078.

[15] Vieira, F., Santana, E.P., Jesus, M., Santos, J., Pires, P., Vaz-velho, M., Silva, D.P., Ruzene, D.S. (2024). Coconut Waste: Discovering Sustainable Approaches to Advance a Circular Economy. *Sustainability*, 16(3066), 1–25. DOI: 10.3390/su16073066

[16] Mankar, A.R., Pandey, A., Pant, K.K. (2022). Microwave-assisted extraction of lignin from coconut coir using deep eutectic solvents and its valorization to aromatics. *Bioresource Technology*, 345, 126528. DOI: 10.1016/j.biortech.2021.126528.

[17] Anuchi, S.O., Campbell, K.L.S., Hallett, J.P. (2022). Effective pretreatment of lignin-rich coconut wastes using a low-cost ionic liquid. *Scientific Reports*, 12(1), 1–11. DOI: 10.1038/s41598-022-09629-4.

[18] Sun, S.C., Xu, Y., Ma, C.Y., Zhang, C., Zuo, C., Sun, D., Wen, J.L., Yuan, T.Q. (2023). Green and efficient fractionation of bamboo biomass via synergistic hydrothermal-alkaline deep eutectic solvents pretreatment: Valorization of carbohydrates. *Renewable Energy*, 217, 119175. DOI: 10.1016/j.renene.2023.119175.

[19] Ismail, K.S.K., Matano, Y., Sakihama, Y., Inokuma, K., Nambu, Y., Hasunuma, T., Kondo, A. (2022). Pretreatment of extruded Napier grass by hydrothermal process with dilute sulfuric acid and fermentation using a cellulose-hydrolyzing and xylose-assimilating yeast for ethanol production. *Bioresource Technology*, 343, 126071. DOI: 10.1016/j.biortech.2021.126071.

[20] Guo, H., Zhao, Y., Chang, J.S., Lee, D.J. (2022). Inhibitor formation and detoxification during lignocellulose biorefinery: A review. *Bioresource Technology*, 361, 127666. DOI: 10.1016/j.biortech.2022.127666.

[21] Kinenge, M.M., Gogate, P.R. (2022). Intensification of alkaline delignification of sugarcane bagasse using ultrasound assisted approach. *Ultrasonics Sonochemistry*, 82, 105870. DOI: 10.1016/j.ultsonch.2021.105870.

[22] Zhang, R., Gao, H., Wang, Y., He, B., Lu, J., Zhu, W., Peng, L., Wang, Y. (2023). Challenges and perspectives of green-like lignocellulose pretreatments selectable for low-cost biofuels and high-value bioproduction. *Bioresource Technology*, 369, 128315. DOI: 10.1016/j.biortech.2022.128315.

[23] Moodley, P., Sewsynker-Sukai, Y., Gueguim Kana, E.B. (2020). Progress in the development of alkali and metal salt catalysed lignocellulosic pretreatment regimes: Potential for bioethanol production. *Bioresource Technology*, 310, 123372. DOI: 10.1016/j.biortech.2020.123372.

[24] Tang, W., Huang, C., Ling, Z., Lai, C., Yong, Q. (2022). Efficient utilization of waste wheat straw through humic acid and ferric chloride co-assisted hydrothermal pretreatment for fermentation to produce bioethanol. *Bioresource Technology*, 364, 128059. DOI: 10.1016/j.biortech.2022.128059.

[25] Tang, W., Wu, X., Huang, C., Ling, Z., Lai, C., Yong, Q. (2021). Revealing the influence of metallic chlorides pretreatment on chemical structures of lignin and enzymatic hydrolysis of waste wheat straw. *Bioresource Technology*, 342, 125983. DOI: 10.1016/j.biortech.2021.125983.

[26] Chen, W.-H., Nižetić, S., Sirohi, R., Huang, Z., Luque, R., M.Papadopoulos, A., Sakthivel, R., Phuong Nguyen, X., Tuan Hoang, A. (2022). Liquid hot water as sustainable biomass pretreatment technique for bioenergy production: A review. *Bioresource Technology*, 344, 126207. DOI: 10.1016/j.biortech.2021.126207.

[27] Tang, W., Wu, X., Huang, C., Ling, Z., Lai, C., Yong, Q. (2021). Comprehensive understanding of the effects of metallic cations on enzymatic hydrolysis of humic acid-pretreated waste wheat straw. *Biotechnology for Biofuels*, 14(1), 25. DOI: 10.1186/s13068-021-01874-5.

[28] Sangadji, N.L., Wijaya, C., Sangian, H.F., Widjaja, A. (2024). Optimization of Ultrasound-enhanced Subcritical Water Hydrolysis of Oil Palm Empty Fruit Bunch for the Production of Fermentable Sugar. *Periodica Polytechnica Chemical Engineering*, 68(2), 203–215. DOI: 10.3311/PPch.23183.

[29] Zhu, W., Houtman, C.J., Zhu, J.Y., Gleisner, R., Chen, K.F. (2012). Quantitative predictions of bioconversion of aspen by dilute acid and SPORL pretreatments using a unified combined hydrolysis factor (CHF). *Process Biochemistry*, 47(5), 785–791. DOI: 10.1016/j.procbio.2012.02.012.

[30] Springer, E.L. (1966). Hydrolysis of aspenwood xylan with aqueous solutions of hydrochloric acid. *Tappi*, 49(3), 102-106.

[31] Jiang, X., Zhai, R., Li, H., Li, C., Deng, Q., Jin, M. (2023). Understanding acid hydrolysis of corn stover during densification pretreatment for quantitative predictions of enzymatic hydrolysis efficiency using modified pretreatment severity factor. *Bioresource Technology*, 386, 129487. DOI: 10.1016/j.biortech.2023.129487.

[32] Ma, Q., Zhu, J., Gleisner, R., Yang, R., Zhu, J.Y. (2018). Valorization of Wheat Straw Using a Recyclable Hydrotrope at Low Temperatures ( $\leq 90$  °C). *ACS Sustainable Chemistry and Engineering*, 6(11), 14480–14489. DOI: 10.1021/acssuschemeng.8b03135.

[33] Huo, D., Sun, Y., Yang, Q., Zhang, F., Fang, G., Zhu, H., Liu, Y. (2023). Selective degradation of hemicellulose and lignin for improving enzymolysis efficiency via pretreatment using deep eutectic solvents. *Bioresource Technology*, 376, 128937. DOI: 10.1016/j.biortech.2023.128937.

[34] Tang, Z., Wu, C., Tang, W., Huang, M., Ma, C., He, Y.-C. (2023). Enhancing enzymatic saccharification of sunflower straw through optimal tartaric acid hydrothermal pretreatment. *Bioresource Technology*, 385, 129279. DOI: 10.1016/j.biortech.2023.129279.

[35] Sluiter, A. (2008). Determination of Structural Carbohydrates and Lignin in Biomass. Laboratory Analytical Procedure (LAP)/National Renewable Energy Laboratory

[36] Fatmawati, A., Nurtono, T., Widjaja, A. (2023). Thermogravimetric kinetic-based computation of raw and pretreated coconut husk powder lignocellulosic composition. *Bioresource Technology Reports*, 22, 101500. DOI: 10.1016/j.biteb.2023.101500.

[37] Sangadji, N.L., Wijaya, C., Muharja, M., Sangian, H.F., Widjaja, A. (2024). Elevated enzymatic hydrolysis by optimization of ultrasonication pretreatment of oil palm empty fruit bunch for glucose production. *Biomass Convers. Biorefin.* 15, 16541–16551. DOI: 10.1007/s13399-024-06430-3

[38] Gong, W.H., Zhang, C., He, J.W., Gao, Y.Y., Li, Y.J., Zhu, M.Q., Wen, J.L. (2022). A synergistic hydrothermal-deep eutectic solvents (DES) pretreatment for acquiring xylooligosaccharides and lignin nanoparticles from Eucommia ulmoides wood. *International Journal of Biological Macromolecules*, 209, 188–197. DOI: 10.1016/j.ijbiomac.2022.04.008.

[39] Ma, C.Y., Xu, L.H., Zhang, C., Guo, K.N., Yuan, T.Q., Wen, J.L. (2021). A synergistic hydrothermal-deep eutectic solvent (DES) pretreatment for rapid fractionation and targeted valorization of hemicelluloses and cellulose from poplar wood. *Bioresource Technology*, 341(July), 125828. DOI: 10.1016/j.biortech.2021.125828.

[40] Kawamura, K., Sako, K., Ogata, T., Mine, T., Tanabe, K. (2020). Production of 5'-hydroxymethylfurfural by the hydrothermal treatment of cotton fabric wastes using a pilot-plant scale flow reactor. *Bioresource Technology Reports*, 11, 100476. DOI: 10.1016/j.biteb.2020.100476.

[41] Sun, Z., Xie, Y., Wei, C., Wang, F., Zhang, Y., Song, F., Cui, H. (2023). Effect of salt addition on cellulose conversion into 5-hydroxymethylfurfural in metal chloride aqueous solution. *Journal of Molecular Liquids*, 383, 122132. DOI: 10.1016/j.molliq.2023.122132.

[42] Gao, K., Chen, Y., Wang, H., Quan, X., Chu, J., Zhang, J. (2023). Production of Xylooligosaccharides and Monosaccharides from Switchgrass by FeCl<sub>3</sub> Hydrolysis Combined with Sodium Perborate Pretreatment. *Bioenergy Research*, 16(4), 2242–2252. DOI: 10.1007/s12155-023-10573-y.

[43] López-Linares, J.C., Romero, I., Moya, M., Cara, C., Ruiz, E., Castro, E. (2013). Pretreatment of olive tree biomass with FeCl<sub>3</sub> prior enzymatic hydrolysis. *Bioresource Technology*, 128, 180–187. DOI: 10.1016/j.biortech.2012.10.076.

[44] Østby, H., Várnai, A. (2023). Hemicellulolytic enzymes in lignocellulose processing. *Essays in Biochemistry*, 67(3), 533–550. DOI: 10.1042/EBC20220154.

[45] Zhang, X., Zhang, W., Lei, F., Yang, S., Jiang, J. (2020). Coproduction of xylooligosaccharides and fermentable sugars from sugarcane bagasse by seawater hydrothermal pretreatment. *Bioresource Technology*, 309, 123385. DOI: 10.1016/j.biortech.2020.123385.

[46] Huang, K., Das, L., Guo, J., Xu, Y. (2019). Catalytic valorization of hardwood for enhanced xylose-hydrolysate recovery and cellulose enzymatic efficiency via synergistic effect of Fe<sup>3+</sup> and acetic acid. *Biotechnology for Biofuels*, 12(1). DOI: 10.1186/s13068-019-1587-4.

[47] Kumar, B., Bhardwaj, N., Verma, P. (2019). Pretreatment of rice straw using microwave assisted FeCl<sub>3</sub>-H<sub>3</sub>PO<sub>4</sub> system for ethanol and oligosaccharides generation. *Bioresource Technology Reports*, 7, 100295. DOI: 10.1016/j.biteb.2019.100295.

[48] Zhu, L., Tang, W., Ma, C., He, Y.-C. (2023). Efficient co-production of reducing sugars and xylooligosaccharides via clean hydrothermal pretreatment of rape straw. *Bioresource Technology*, 388, 129727. DOI: 10.1016/j.biortech.2023.129727.

[49] Yue, P., Hu, Y., Tian, R., Bian, J., Peng, F. (2022). Hydrothermal pretreatment for the production of oligosaccharides: A review. *Bioresour. Technol.* 343, 126075. DOI: 10.1016/j.biortech.2021.126075

[50] Freitas, V., Paez, A., Fongarland, P., Philippe, R., Vilcoq, L. (2023). Catalytic hydrogenation of hemicellulosic sugars: reaction kinetics and influence of sugar structure on reaction rate, *ChemCatChem*, 15, 13, e202300263. DOI: 10.1002/cctc.202300263.

[51] Zhao, J., Li, J., Qi, G., Sun, X.S., Wang, D. (2021). Two Nonnegligible Factors Influencing Lignocellulosic Biomass Valorization: Filtration Method after Pretreatment and Solid Loading during Enzymatic Hydrolysis. *Energy and Fuels*, 35 (2), 1546–1556. DOI: 10.1021/acs.energyfuels.0c03876.

[52] Xia, Q., Liu, Y., Meng, J., Cheng, W., Chen, W., Liu, S., Liu, Y., Li, J., Yu, H. (2018). Multiple hydrogen bond coordination in three-constituent deep eutectic solvents enhances lignin fractionation from biomass. *Green Chemistry*, 20(12), 2711–2721. DOI: 10.1039/c8gc00900g.

[53] Kamireddy, S.R., Li, J., Tucker, M., Degenstein, J., Ji, Y. (2013). Effects and Mechanism of Metal Chloride Salts on Pretreatment and Enzymatic Digestibility of Corn Stover. *Industrial & Engineering Chemistry Research*, 52(5), 1775–1782. DOI: 10.1021/ie3019609.

[54] Lu, X., Gu, X., Shi, Y. (2022). A review on lignin antioxidants: Their sources, isolations, antioxidant activities and various applications. *Int. J. Biol. Macromol.* 210, 716–741. DOI: 10.1016/j.ijbiomac.2022.04.228

[55] Hong, S., Sun, X., Lian, H., Pojman, J.A., Mota-Morales, J.D. (2020). Zinc chloride/acetamide deep eutectic solvent-mediated fractionation of lignin produces high- and low-molecular-weight fillers for phenol-formaldehyde resins. *Journal of Applied Polymer Science*, 137 (7), 48385. DOI: 10.1002/app.48385.

[56] Wang, R., Wang, K., Zhou, M., Xu, J., Jiang, J. (2021). Efficient fractionation of moso bamboo by synergistic hydrothermal-deep eutectic solvents pretreatment. *Bioresource Technology*, 328 (January), 124873. DOI: 10.1016/j.biortech.2021.124873.

[57] Huo, D., Sun, Y., Yang, Q., Zhang, F., Fang, G., Zhu, H., Liu, Y. (2023). Selective degradation of hemicellulose and lignin for improving enzymolysis efficiency via pretreatment using deep eutectic solvents. *Bioresource Technology*, 376, 128937. DOI: 10.1016/j.biortech.2023.128937.

[58] Kamireddy, S.R., Li, J., Tucker, M., Degenstein, J., Ji, Y. (2013). Effects and mechanism of metal chloride salts on pretreatment and enzymatic digestibility of corn stover. *Industrial and Engineering Chemistry Research*, 52(5), 1775–1782. DOI: 10.1021/ie3019609.

[59] Ji, H., Song, Y., Zhang, X., Tan, T. (2017). Using a combined hydrolysis factor to balance enzymatic saccharification and the structural characteristics of lignin during pretreatment of Hybrid poplar with a fully recyclable solid acid. *Bioresource Technology*, 238, 575–581. DOI: 10.1016/j.biortech.2017.04.092.

[60] Zhou, M., Lv, M., Cai, S., Tian, X. (2023). Effects of enzymatic hydrolysis and physicochemical properties of lignocellulose waste through different choline based deep eutectic solvents (DESSs) pretreatment. *Industrial Crops and Products*, 195, 116435. DOI: 10.1016/j.indcrop.2023.116435.

[61] Shen, X.J., Wen, J.L., Mei, Q.Q., Chen, X., Sun, D., Yuan, T.Q., Sun, R.C. (2019). Facile fractionation of lignocelluloses by biomass-derived deep eutectic solvent (DES) pretreatment for cellulose enzymatic hydrolysis and lignin valorization. *Green Chemistry*, 21(2), 275–283. DOI: 10.1039/c8gc03064b.

[62] Jose, S., Sajeena Beevi, B. (2023). Optimization of ultrasonication assisted alkaline delignification of coir pith using response surface methodology. *Bioresource Technology Reports*, 21, 101330. DOI: 10.1016/j.biteb.2023.101330.

[63] Sunar, S.L., Oruganti, R.K., Bhattacharyya, D., Shee, D., Panda, T.K. (2024). Deep eutectic solvent pretreatment of sugarcane bagasse for efficient lignin recovery and enhanced enzymatic hydrolysis. *Journal of Industrial and Engineering Chemistry*, 139, 539–553. DOI: 10.1016/j.jiec.2024.05.030

[64] Xu, H., Che, X., Ding, Y., Kong, Y., Li, B., Tian, W. (2019). Effect of crystallinity on pretreatment and enzymatic hydrolysis of lignocellulosic biomass based on multivariate analysis. *Bioresource Technology*, 279, 271–280. DOI: 10.1016/j.biortech.2018.12.096.

[65] Shen, B., Hou, S., Jia, Y., Yang, C., Su, Y., Ling, Z., Huang, C., Lai, C., Yong, Q. (2021). Synergistic effects of hydrothermal and deep eutectic solvent pretreatment on co-production of xylo-oligosaccharides and enzymatic hydrolysis of poplar. *Bioresource Technology*, 341(July), 125787. DOI: 10.1016/j.biortech.2021.125787.

[66] Ruiz, H.A., Sganzerla, W.G., Larnaudie, V., Veersma, R.J., van Erven, G., Shiva, Ríos-González, L.J., Rodríguez-Jasso, R.M., Rosero-Chasoy, G., Ferrari, M.D., Kabel, M.A., Forster-Carneiro, T., Lareo, C. (2023). Advances in process design, techno-economic assessment and environmental aspects for hydrothermal pretreatment in the fractionation of biomass under biorefinery concept. *Bioresour. Technol.* 369, 128469. DOI: 10.1016/j.biortech.2022.128469.

[67] Gandam, P.K., Chinta, M.L., Pabbathi, N.P.P., Baadhe, R.R., Sharma, M., Thakur, V.K., Sharma, G.D., Ranjitha, J., Gupta, V.K. (2022). Second-generation bioethanol production from corncob – A comprehensive review on pretreatment and bioconversion strategies, including techno-economic and lifecycle perspective. *Industrial Crops and Products*, 186, 115245. DOI: 10.1016/j.indcrop.2022.115245.

[68] Neves, P. V., Pitarelo, A.P., Ramos, L.P. (2016). Production of cellulosic ethanol from sugarcane bagasse by steam explosion: Effect of extractives content, acid catalysis and different fermentation technologies. *Bioresource Technology*, 208, 184–194. DOI: 10.1016/j.biortech.2016.02.085.

[69] Sarker, T.R., Pattnaik, F., Nanda, S., Dalai, A.K., Meda, V., Naik, S. (2021). Hydrothermal pretreatment technologies for lignocellulosic biomass: A review of steam explosion and subcritical water hydrolysis. *Chemosphere*, 284, 131372. DOI: 10.1016/j.chemosphere.2021.131372.

[70] Prado, J.M., Forster-Carneiro, T., Rostagno, M.A., Follegatti-Romero, L.A., Maugeri Filho, F., Meireles, M.A.A. (2014). Obtaining sugars from coconut husk, defatted grape seed, and pressed palm fiber by hydrolysis with subcritical water. *Journal of Supercritical Fluids*, 89, 89–98. DOI: 10.1016/j.supflu.2014.02.017.

[71] Ren, Y., Si, B., Liu, Z., Jiang, W., Zhang, Y. (2022). Promoting dark fermentation for biohydrogen production: Potential roles of iron-based additives. *International Journal of Hydrogen Energy*, 47(3), 1499–1515. DOI: 10.1016/j.ijhydene.2021.10.137.

[72] Singh, A., Tsai, M.L., Chen, C.W., Rani Singhania, R., Kumar Patel, A., Tambat, V., Dong, C. Di, (2023). Role of hydrothermal pretreatment towards sustainable biorefinery. *Bioresource Technology*, 367, 128271. DOI: 10.1016/j.biortech.2022.128271.

[73] Muharja, M., Umam, D.K., Pertiwi, D., Zuhdan, J., Nurtono, T., Widjaja, A. (2019). Enhancement of sugar production from coconut husk based on the impact of the combination of surfactant-assisted subcritical water and enzymatic hydrolysis. *Bioresource Technology*, 274(November 2018), 89–96. DOI: 10.1016/j.biortech.2018.11.074.

[74] Xiong, H., Liu, Y., Xu, Q. (2020). Effect of sodium dodecyl sulfate on the production of L-isoleucine by the fermentation of *Corynebacterium glutamicum*. *Bioengineered*, 11(1), 1124–1136. DOI: 10.1080/21655979.2020.1831364.

[75] Peng, J., Xu, H., Wang, W., Kong, Y., Su, Z., Li, B. (2021). Techno-economic analysis of bioethanol preparation process via deep eutectic solvent pretreatment. *Industrial Crops and Products*, 172, 114036. DOI: 10.1016/j.indcrop.2021.114036.

[76] Zhang, J., Fan, C., Zang, L. (2017). Improvement of hydrogen production from glucose by ferrous iron and biochar. *Bioresource Technology*, 245 (September), 98–105. DOI: 10.1016/j.biortech.2017.08.198